Research Article

Controlled synthesis of uniform hollow polypyrrole microcapsules by a cosolvent approach

Tsung-Lin Hsieh[1] · Pei-Sung Hung[1] · Chuan-Jyun Wang[1] · Yu-Szu Chou[1] · Pu-Wei Wu[1]

Abstract
A simple and effective synthetic approach is demonstrated for the formation of uniform hollow polypyrrole (PPy) microcapsules. This process entails the preparation of homogeneous polystyrene@polypyrrole (PS@PPy; core@shell) microspheres, followed by chemical extraction of the PS cores. By proper dispersion of monodispersive PS microspheres and pyrrole molecules in a water/ethanol cosolvent to minimize the diffusion of pyrrole molecules to the PS microspheres, we are able to prepare uniform PS@PPy microspheres with significantly reduced size variation, deformation, and aggregation. The PS microspheres, in diameter of 490 nm, carry negative surface charges, and after the deposition of PPy, reveal a transition from positive to negative surface charges with increasing pH values. The hollow PPy microcapsules, in diameter of 527 nm and shell thickness of 20 nm, are fabricated after selective removal of PS cores from the PS@PPy microspheres in tetrahydrofuran. Analysis tools including Fourier transform infrared spectroscopy, thermogravimetric analyzer, and zeta potential, as well as scanning and transmission electron microscopes are employed for material characterization.

Keywords Core–shell · Hollow microcapsule · Polystyrene · Polypyrrole · Microsphere · Cosolvent

1 Introduction

Since the first observation of conductive behavior in halogen-doped polyacetylene in 1977, there has been significant interests to explore conductive polymers for their unique physical and chemical properties [1]. The attributes that render these conducting polymers attractive include tunable electrical conductivity, structural flexibility, and processing adaptability. To date, a variety of conductive polymers including polyaniline, poly(3,4-ethylenedioxythiophene), polyacetylene, and polypyrrole (PPy) have been synthesized and studied with various success [2–6]. Among them, the PPy has attracted the most attention because of its impressive electrical, electrochemical, and optical characteristics, as well as excellent environmental stability. Among many forms of PPy, the hollow PPy microcapsules are of particular interest for promising potentials in rechargeable batteries, supercapacitors, and electrocatalyst supports [7–10].

Successful formation of hollow PPy microcapsules usually entails a template approach in which a sacrificial core is used to prepare a core@shell microsphere, followed by the selective removal of the core. For examples, core@PPy microspheres have been prepared for applications in biosensors, visual biomedical diagnostics, fuel cells, catalysis, and absorbers for electromagnetic waves [10–19]. In the literatures, the widely studied cores are silica and polystyrene (PS) microspheres [20–27]. Between them, the PS microspheres are recognized for a wider processing window, more freedoms in size availability and uniformity, as well as easier to be selectively removed by either chemical extraction or combustion.

During the synthesis of core@PPy microspheres, it is recognized that uniform and well-defined spherical core@PPy microspheres are difficult to obtain. So far, several

✉ Pu-Wei Wu, ppwu@mail.nctu.edu.tw | [1]Department of Materials Science and Engineering, National Chiao Tung University, Hsinchu 300, Taiwan, ROC.

SN Applied Sciences (2019) 1:319 | https://doi.org/10.1007/s42452-019-0332-8

Received: 14 February 2019 / Accepted: 3 March 2019 / Published online: 8 March 2019

groups have investigated relevant processing parameters responsible for the morphology formation during core@PPy synthesis. For instance, Yang et al. [20] reported that a pre-treatment of silica with different modified agents was critical for better morphology control in silica@PPy. In addition, Huang et al. [28] proposed an "inside-out" approach to prepare PS@PPy microspheres in which the pyrrole monomers were pre-absorbed inside the PS microspheres, followed by a drive-out step to render the polymerization of pyrrole on the PS surface. In their study, they observed that the morphology for PS@PPy microspheres was affected by varying the PS/pyrrole weight ratio or the addition rate of acid. Another study on the effect of hydrophilicity of the core during PPy formation by Cairns et al. [29] indicated that a better PPy coating was achieved on a hydrophobic poly(n-butyl methacrylate) (PBMA) surface instead of a hydrophilic poly(methyl methacrylate) (PMMA) one. To the best of our knowledge, however, the adjustment of chemical affinity of pyrrole monomers in an aqueous solution by the addition of organic solvent to control the resulting morphology of PS@PPy microspheres has not been investigated yet.

In this work, we employed a cosolvent approach to determine the optimized water/ethanol ratio for the formation of homogeneous PS@PPy microspheres. The effect of water/ethanol volume ratio was carefully studied with comprehensive physical and materials characterization. Subsequently, a chemical extraction process was adopted to produce uniform hollow PPy microcapsules.

2 Materials and method

2.1 Synthesis of PS and PS@PPy microspheres

PS microspheres with an average diameter of 490 nm were synthesized via an emulsifier-free emulsion polymerization process. The synthesis was conducted in a batch reactor equipped with a bladed pitched paddle impeller. The reactor contained 2 L DI water and was deoxygenated under N_2 at 65 °C for 12 h. Then, styrene (monomer), $C_8H_7NaO_3S$ (co-monomer), and $NaHCO_3$ (buffer) were mixed to form a homogeneous solution. After 15 min, $K_2S_2O_8$ (initiator) was added, followed by stirring at 370 rpm for 16 h before cooling to 25 °C. Subsequently, the mixture was immersed in a water bath at 65 °C to evaporate residual solvent, resulting in PS microspheres in white powdery form.

To synthesize PS@PPy microspheres, 0.6 g PS microspheres and 0.1 g poly(N-vinylpyrrolidone) (PNVP; stabilizer) were mixed in 30 mL solution containing different volume ratios of DI water and ethanol (the ethanol volume percentage was varied from 1.5 to 60% whereas the PS/PPy weight ratio was maintained at 2.5). The mixture was subjected to ultrasonication for 4 h at 25 °C. Afterward, 1.6 g $FeCl_3{\cdot}6H_2O$ (oxidant) was dissolved for 1 h, followed by the addition of 249 µL pyrrole (98 wt%) to initiate the polymerization process. The polymerization reaction lasted for 24 h at 25 °C. Subsequently, the sample underwent three centrifugation/re-dispersion cycles during which the supernatants were replaced with DI water in order to remove residual inorganic by-products ($FeCl_2$ and HCl). The resulting dispersion was dried at 60 °C for 12 h to obtain PS@PPy microspheres in black powders.

The PNVP, with a nominal molecular weight of 360,000, was purchased from Aldrich and used without further purification. Pyrrole (Alfa) and Styrene (Aldrich) were removed of inhibitor by passing through a column of activated basic alumina prior to use. $FeCl_3{\cdot}6H_2O$ (Aldrich), $K_2S_2O_8$, $C_8H_7NaO_3S$, and $NaHCO_3$ were used as received.

2.2 Formation of hollow PPy microcapsules

Hollow PPy microspheres were fabricated by immersing 10 mg PS@PPy microspheres in 20 mL tetrahydrofuran (THF) under stirring at 25 °C for 24 h to dissolve the PS microspheres. The resulting hollow PPy microcapsules were isolated from THF by centrifugation at 6000 rpm for 15 min, followed by thorough ethanol washing for three times. Lastly, the sample was dried at 50 °C for 12 h before further material characterization. Figure 1 presents the schematic for the synthetic steps involved for the formation of hollow PPy microcapsules.

2.3 Materials characterization

A scanning electron microscope (SEM; JEOL-LSM-6700) was used to observe morphologies of PS and PS@PPy microspheres, as well as hollow PPy microcapsules, respectively. To prepare SEM specimen, the samples were casted onto an ITO glass, followed by a Pt sputtering. Afterward, the specimens were maintained under 9.63×10^{-5} Pa, and the SEM observation entailed an acceleration voltage of 15 kV with an emission current of 10 µA. A transmission electron microscope (TEM; Philips/FEI TECNAI 20) was employed to observe the morphology of hollow PPy microcapsules. To prepare TEM specimen, the sample was dropped onto a copper grid, and residual solvent was evaporated at 60 °C for 12 h. Fourier transform infrared (FTIR) analysis was performed to validate the diffusion of pyrrole molecules to PS microspheres and the FTIR spectra were obtained using a FTIR spectrometer (PerkinElmer spectrum 100) in N_2 atmosphere. Thermogravimetric analysis (TGA; TA Instruments Q500) was conducted to determine the exact amount of PPy in PS@PPy microspheres. The heating rate was 10 °C min^{-1} from 25 to 800 °C in N_2

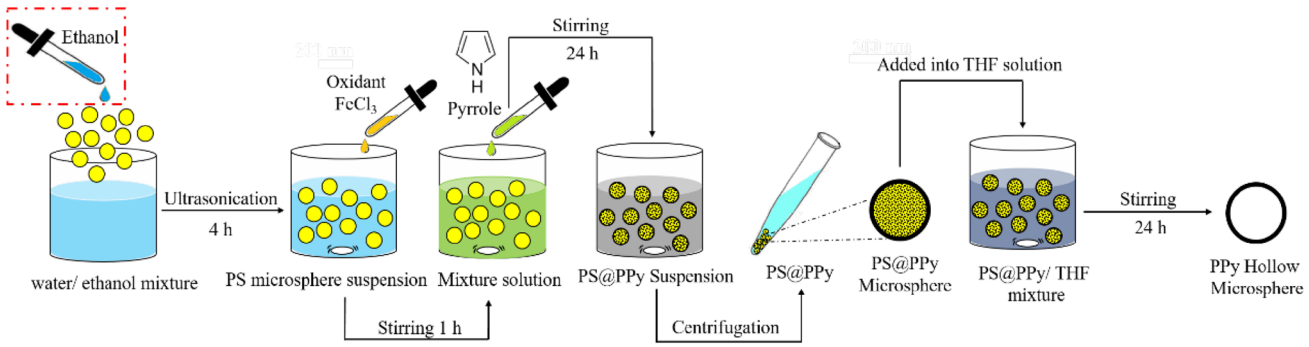

Fig. 1 A schematic for the synthetic steps involved for the fabrication of PS@PPy microspheres and hollow PPy microcapsules

atmosphere. The zeta potential and polydispersity of PS and PS@PPy microspheres were determined via a particle analyzer (Beckman Coulter, Delsa Nano C). For zeta potential measurements, the pH value for the dispersion was adjusted by 0.1 M HCl and NaOH aqueous solution.

3 Results and discussion

Successful fabrication of uniform hollow PPy microcapsules requires monodispersive PS microspheres as the template with consistent coating of PPy. Therefore, the processing steps for the synthesis of homogeneous PS@PPy microspheres becomes rather critical. Figure 2a, b

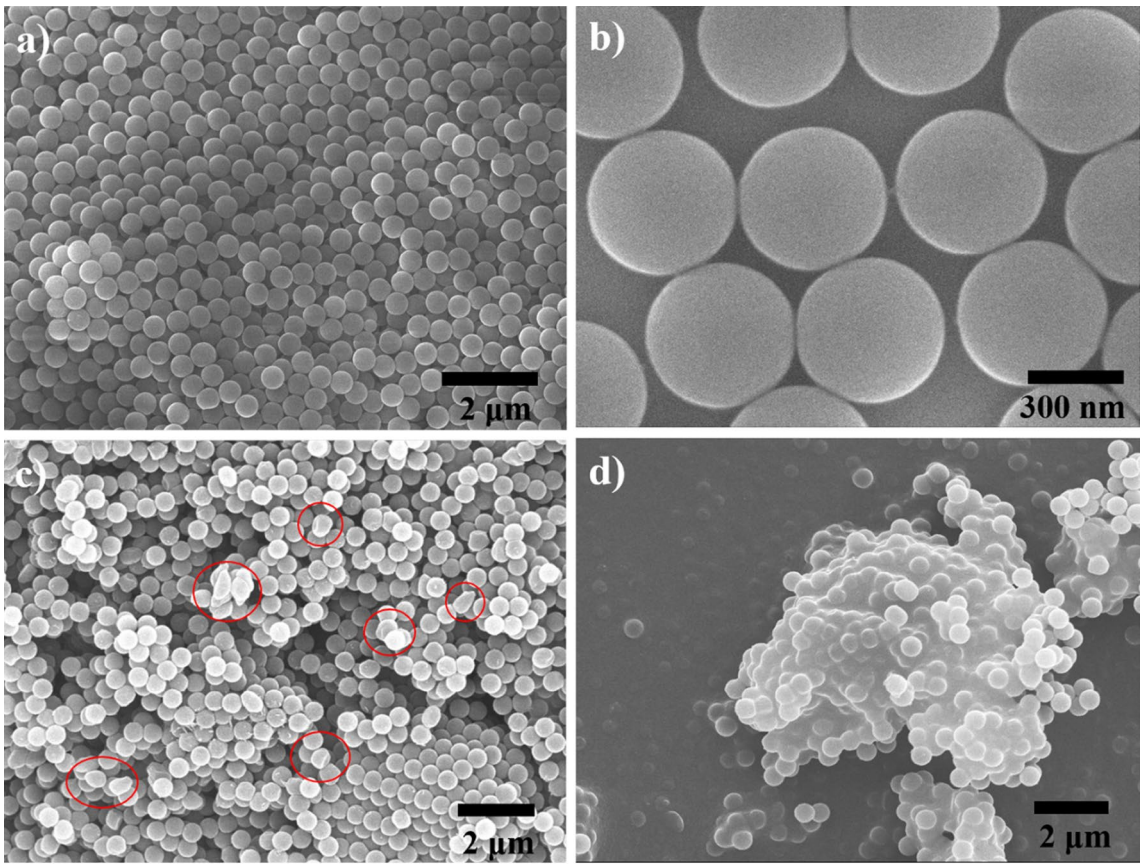

Fig. 2 The SEM images of PS microspheres in **a** low and **b** high magnification, as well as PS@PPy microspheres showing **c** deformations (as indicated in red circles) and **d** sever aggregation. These PS@PPy microspheres are synthesized without the addition of ethanol

exhibit the SEM images of PS microspheres in low and high magnification. As shown, the PS microspheres appeared in spherical shape with a smooth surface morphology. In addition, their size was rather consistent and the average diameter was 490 nm with a standard deviation of 7.4 nm. It is to be noted that we did not observe any deformation as our synthetic process was rather robust and reproducible. However, the PS@PPy microspheres synthesized without the addition of ethanol revealed considerable deformation, as indicated in red circles in Fig. 2c. We believed that the formation of deformed PS@PPy microspheres was due to the diffusion of pyrrole molecules into the PS microspheres during the synthetic stage as both PS microspheres and pyrrole molecules are hydrophobic in nature. Therefore, in an aqueous medium, the pyrrole molecules preferred to stay with PS microspheres instead of dispensing in water. As a result, the pyrrole molecules acted as a plasticizer in softening the PS microsphere, causing the latter to deform moderately. Moreover, since those individual PS microspheres were not dispersed well in an aqueous solution, they tended to aggregate into large assembly. Thus, during the polymerization of pyrrole molecules, the PPy also covered and bonded those individual PS microspheres together, leading to irregularly-shaped agglomerates with sizes larger than 10 µm, as shown in Fig. 2d.

In order to validate the diffusion of pyrrole molecules to PS microspheres during our synthetic step, we obtained FTIR spectra from PNVP-stabilized PS microspheres and pyrrole molecules, as well as sample with identical formulation of PS@PPy microspheres except without the addition of $FeCl_3 \cdot 6H_2O$ (labeled as PS-pyrrole in Fig. 3). This ensured that the polymerization of pyrrole molecules was not taking place so the individual pyrrole molecules were still entrapped in the PS microspheres. As shown in Fig. 3, there appeared two distinct absorption peaks associated with pyrrole molecules, and they were located at 736 and

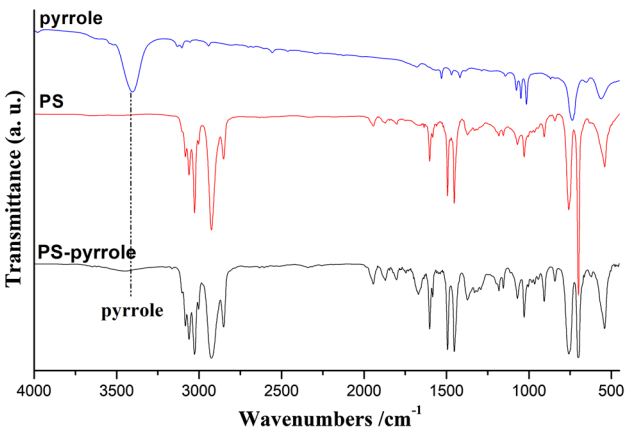

Fig. 3 The FTIR spectra of pyrrole molecules, PNVP-stabilized PS microspheres, and PS microspheres mixed with pyrrole molecules

3404 cm^{-1}, respectively. These two signals corresponded to C=C bending and N–H stretching vibration. The PNVP-stabilized PS microspheres revealed obvious peaks at 699, 1453, 1494, 1602, 2929, and 3027 cm^{-1} from PS microspheres, as well as 1670 cm^{-1} from the pyrrolidone carbonyl group of PNVP. It is noted that our results agreed well with what was reported in earlier literature [22]. From the pyrrole-PS FTIR profile, we observed an identical pattern like PNVP-stabilized PS microspheres. In addition, a subdued absorption peak around 3440 cm^{-1} was recorded. This confirmed the presence of pyrrole molecules, providing a solid evidence about the diffusion of pyrrole molecules to the PS microspheres in an aqueous solution. A similar pattern was reported earlier by Huang et al. [28] in which a gradual disappearance of pyrrole molecular droplets after mixing pyrrole molecules and PS microspheres in an aqueous solution was observed under optical microscope observation. In addition, according to Zhang et al., the diffusion of pyrrole molecules to PS microspheres was anticipated because the PS microspheres were completely dissolved in pyrrole when the PS microspheres and pyrrole molecules were mixed together [30].

To reduce undesirable deformation and aggregation of PS@PPy microspheres, ethanol was adopted as a cosolvent because the ethanol not only is miscible with water, but also exhibits greater affinity toward both pyrrole molecules and PS microspheres. With the presence of ethanol, we expected the pyrrole molecules to remain in the liquid phase rather than diffusing into the PS microspheres (organic phase). In addition, using ethanol as a cosolvent, the PS microspheres were likely to disperse more uniformly in the mixture. Both features suggested the feasibility of fabricating PS@PPy microspheres with significantly reduced deformation.

A series of PS@PPy microspheres were synthesized by varying the ethanol volume percentage from 1.5 to 60% while keeping the PS/pyrrole weight ratio at 2.5. The resulting SEM images are provided in Fig. 4. Apparently, a lower ethanol volume percentage of 1.5–10% engendered PS@PPy microspheres in spherical shape with subdued deformation and aggregation (shown in Fig. 4a–d). In contrast, with an ethanol volume percentage of 15% and above, there appeared noticeable irregularly-shaped PS@PPy microspheres (shown in Fig. 4e–h). However, the undesirable aggregation pattern was mostly inhibited as long as ethanol was added. In short, the optimized formula for fabricating homogeneous PS@PPy microspheres with significantly reduced deformation was 7 vol% of ethanol.

To quantitatively determine the deformation ratio of PS@PPy microspheres synthesized from various volume percentages of ethanol, we selected 18 SEM images at 10,000 magnification from each sample, and calculated the number of deformed PS@PPy and un-deformed PS@

PPy microspheres, respectively. To define a deformed PS@PPy microsphere, we first determined *a* (the longest diameter of a PS@PPy microsphere) and *b* (the shortest diameter of the same PS@PPy microsphere). Then, the *x* was obtained using the following equation;

$$x = \left[(a-b)/\left(\frac{a+b}{2}\right)\right] \quad (1)$$

where the *x* is a parameter indicative of deformation degree, and any PS@PPy microsphere with *x* larger than 7% is defined as a deformed PS@PPy microsphere. The deformation ratio, shown in Fig. 5 (left Y-axis), was then determined by dividing the number of deformed PS@PPy microspheres by the total number of PS@PPy microspheres in those 18 SEM images. Apparently, the deformation ratio was substantially reduced from 7 to 3.5 vol%.

Chemically, the affinity of the pyrrole molecule is ethanol > PS microsphere > water. Therefore, we believed that a small amount of ethanol enables the pyrrole molecules to remain in the liquid medium instead of diffusing to the PS microspheres. At the same time, the PS microspheres became partially dispersible in the solution after ethanol was added. Consequently, severe aggregation of PS microspheres was avoided and the pyrrole molecules were able to polymerize on the PS microspheres forming the desirable PS@PPy microstructure. However, with the ethanol volume percentage reached 15 vol% and above, the PS microspheres and pyrrole molecules were mixed homogeneously in the mixture. As a result, the diffusion of pyrrole molecules to the PS microspheres took place again. This led to moderate increase in the number of deformed PS@PPy microspheres but at the same time, the extent of aggregation was still negligible. It is noted that the ethanol and water are totally miscible. Therefore, we were unable to observe any noticeable phase change associated with the re-distribution of PS microspheres and pyrrole molecules in the water/ethanol mixture.

The polydispersity of PS@PPy microspheres synthesized with different volume percentages of ethanol is also presented in Fig. 5 (right Y-axis). By definition, the polydispersity was obtained using the following equation;

$$\mathrm{PDI} = \left(\frac{s}{\bar{x}}\right)^{\frac{1}{2}} \quad (2)$$

where the *s* is the standard deviation of PS@PPy microspheres, and the $\bar{x}$ is the average diameter of PS@PPy microspheres. For the as-synthesized PS microspheres, its polydispersity was 0.093, indicating its monodispersive nature. In contrast, the polydispersity of PS@PPy microspheres was above 0.1 and became larger with increasing ethanol amount. It was reasonable to expect a larger value of polydispersity once a PPy layer was deposited on the PS microspheres. Among these samples, the PS@PPy microspheres synthesized with 3.5 vol% of ethanol revealed the lowest polydispersity.

The average thickness of PPy shell for the PS@PPy microspheres was obtained by measuring the diameter of PS@PPy microspheres from SEM images, and subtrating that value by 490 nm (the average diameter of PS microsphere). Table 1 lists the average diameter of PS@PPy microspheres (from 50 PS@PPy microspheres) and their respective PPy shell thickness, from samples synthesized with different volume percentages of ethanol. Interestingly, there appeared similar PPy shell thickness among samples synthesized with ethanol volume percentage of 0–7%. For samples with ethanol above 15%, the PPy shell thickness was reduced to some degrees. We rationalized that a thinner PPy shell was attributed to a reduced chemical reactivity of $FeCl_3$ because its solubility in the ethanol/water mixture was decreased with increasing ethanol amount. As a result, the complete polymerization of pyrrole molecules was not achieved leading to a moderate reduction in PPy shell thickness.

We also attempted to estimate the PPy utilization rate (as listed in Table 1) during the synthesis of PS@PPy microspheres by first determining the number of PS microspheres (N_{PS}) used in a batch and the weight of PPy shell for a single PS@PPy microsphere (W_{PPy}). The N_{PS} was obtained by dividing the total weight of PS microspheres (0.6 g) by the weight of a single PS microsphere (W_{PS}). The N_{PS}, W_{PS}, and W_{PPy} for a single PS@PPy microsphere were calculated by following equations;

$$W_{PS} = \frac{4}{3} \times \pi \times r_{ps}^3 \times D_{PS} \quad (3)$$

$$W_{PPy} = \frac{4}{3}\pi\left[\left(r_{PS-PPy}^3\right) - \left(r_{PS}^3\right)\right] \times D_{PPy} \quad (4)$$

$$N_{PS} = \frac{0.6}{W_{PS}} \quad (5)$$

where the r_{PS} and the r_{PS-PPy} are the average radius of PS and PS@PPy microsphere, and the D_{PS} and the D_{PPy} are the density of polystyrene (1.05 g cm^{-3}) and polypyrrole (1.46 g cm^{-3}), respectively. Afterwards, the PPy utilization rate could be estimated by dividing the total weight of PPy shell by the amount of pyrrole (0.24 g) used in a batch as following equation;

$$PPy\ utilization(\%) = \frac{N_{PS} \times W_{PPy}}{0.24} \quad (6)$$

After further simplification, the PPy utilization rate could be obtained in following equation;

$$PPy\ utilization(\%) = \left[\left(\frac{r_{PS-PPy}}{r_{PS}}\right)^3 - 1\right] \times \frac{D_{PPy}}{D_{PS}} \times 2.5 \quad (7)$$

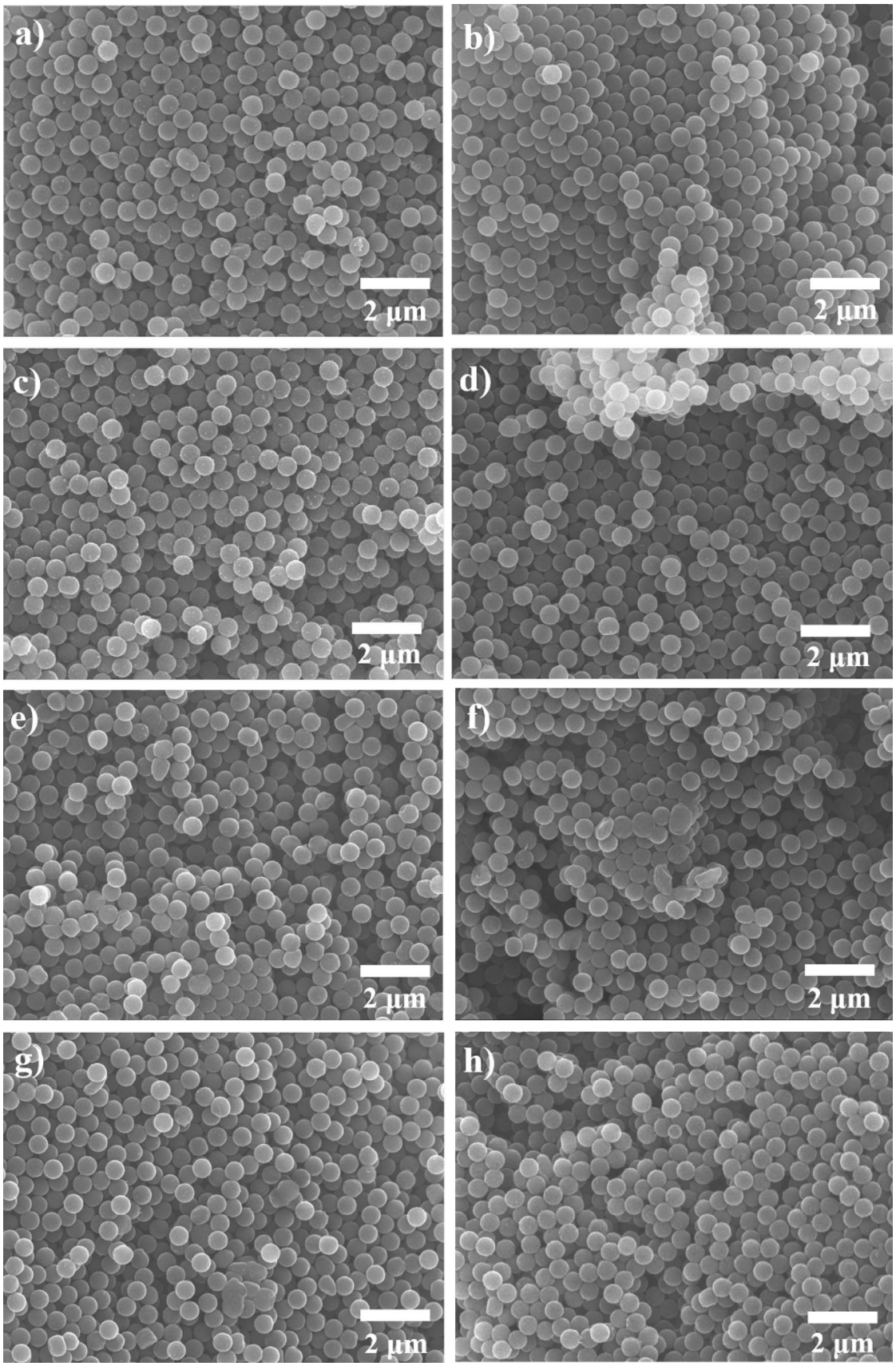
a)
2 µm
b)
2 µm
c)
2 µm
d)
2 µm
e)
2 µm
f)
2 µm
g)
2 µm
h)
2 µm

◂**Fig. 4** The SEM images of PS@PPy microspheres synthesized with different volume percentages of ethanol as a cosolvent: **a** 1.5, **b** 3.5, **c** 7, **d** 10, **e** 15, **f** 30, **g** 45 and **h** 60%

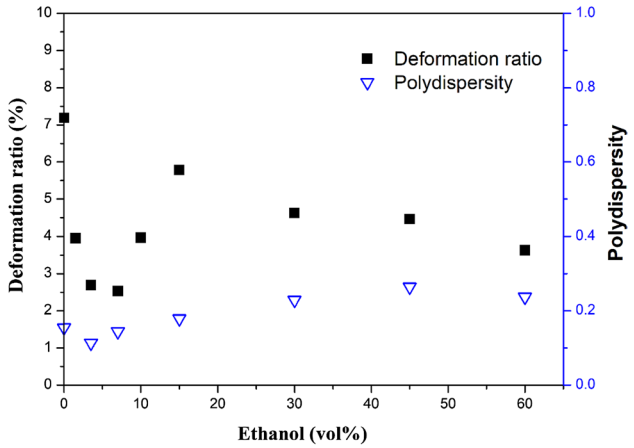

Fig. 5 **a** The deformation ratio (left Y-axis) and polydispersity (right Y-axis) of PS@PPy microspheres synthesized with different volume percentages of ethanol as a cosolvent. **b** The schematic illustrating the distribution of PS microspheres and PPy molecules in a cosolvent with different volume percentages of ethanol

Table 1 Relevant properties of PS@PPy microspheres prepared with different volume percentages of ethanol

Ethanol vol%	Diameter (nm)	Standard deviation	PPy shell thickness (nm)	PPy utilization (%)
0	524	7.4	17	77
1.5	527	8.1	18.5	84
3.5	522	6.3	16	72
7	526	6.8	18	82
10	516	8.7	13	58
15	516	7.8	13	58
30	517	7.9	13.5	60
45	519	8.4	14.5	65
60	517	8.5	13.5	60

The TGA profiles for PS microspheres, as well as PS@PPy microspheres synthesized with ethanol volume percentage of 7 and 15% are provided in Fig. 6. Apparently, these samples revealed a notable weight loss between 300 and 400 °C, which was due to the decomposition of PS microspheres. In addition, the weight loss at 800 °C was 92 and 83% for PS@PPy microspheres synthesized with ethanol volume percentage of 15 (curve b) and 7% ethanol (curve c), respectively. Because the TGA data were recorded in N_2 atmosphere, according to earlier literature [31], the PPy was unable to be decomposed entirely but converted to a carbon-rich substance at elevated temperature. Our TGA

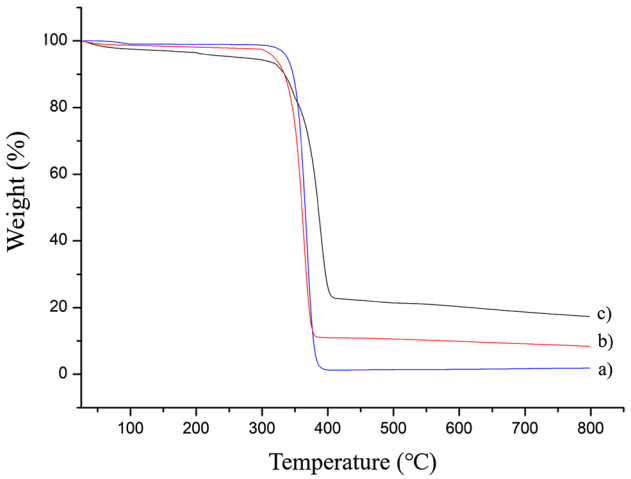

Fig. 6 The TGA curves of (a) PS microspheres, as well as PS@PPy microspheres synthesized with ethanol volume percentage of (b) 15 and (c) 7%, respectively

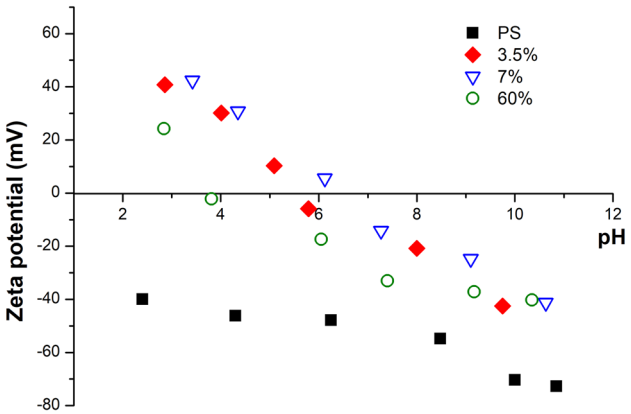

Fig. 7 The zeta potential as a function of pH value for PS microspheres and PS@PPy microspheres synthesized with ethanol volume percentage of 3.5, 7, and 60%

results were consistent with what was reported by Huang et al. in which a ~ 33% weight loss of PPy at 700 °C was observed [28]. In addition, the residual weight of PS@PPy microspheres after the decomposition of PS microspheres represented the exact amount of PPy loading in PS@PPy microspheres. From TGA profiles, the difference in the PPy loading between cure b and c was in reasonable agreement with the thickness difference of PPy shell from PS@PPy microspheres in Table 1.

Figure 7 shows the zeta potential as a funciton of pH for PS microspheres as well as PS@PPy microspheres synthesized with 3.5, 7, and 60 vol% of ethanol. Apparently, the PS microsphere exhibited negative surface charges from pH 2 to pH 11. Its negative charge was attributed to the sulfonate groups from the synthetic stage. In contrast,

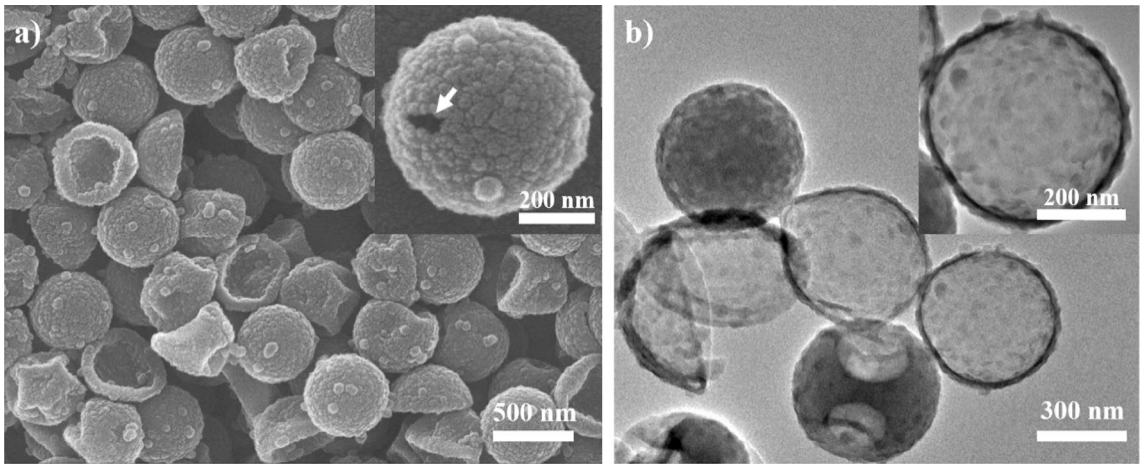

Fig. 8 The **a** SEM and **b** TEM images of PPy hollow microspheres obtained after immersing the PS@PPy microspheres in THF. These PS@PPy microspheres are synthesized with 7 vol% of ethanol as a cosolvent. Inset in **a** shows a hollow PPy microcapsule with a hole on its PPy shell. Inset in **b** shows a representative hollow PPy microcapsule showing the complete removal of PS core

the PS@PPy microsphere revealed a transition from positive surface charges at low pH value to negative surface charges at high pH value. The isoelectric point for the PS@PPy microsphere synthesized with 3.5, 7, and 60 vol% of ethanol was 5.53, 6.44, and 3.73, respectively. According to literature [32], the positive surface charge of PS@PPy microsphere was due to the protonation of nitrogen atoms of polypyrrole and simultaneous dissociation of doped Cl^- ions when the pH value was below its isoelectric point. On the other hand, when the pH value was increased above its isoelectric point, the PS@PPy microsphere demonstrated a negative surface charge attributed to the deprotonation of the protonated nitrogen atoms on polypyrrole and selective adsorption of OH^- ions on the surface of polypyrrole. Notably, the PS@PPy microsphere synthesized with 60 vol% of ethanol exhibited a moderate shift of isoelectric point to a lower pH value as compared to those synthesized with 3.5 and 7 vol% of ethanol. This moderate shift was likely influenced by the thickness of PPy layer as a thicker PPy shell rendered a larger isoelectric point because of less influence from the negative charges on the PS microsphere.

Figure 8a exhibits a SEM image of hollow PPy microcapsules whose average diameter was around 527 nm. Some fractured PPy microspheres were also observed, which confirmed that the THF was able to dissolve the PS microsphere selectively. From the SEM image, upon the removal of PS microspheres, some of the remaining PPy microspheres suffered from structural damage due to lack of mechanical strength from the PPy shell. Inset in Fig. 8a revealed a hollow PPy microcapsule with a surface hole. This image indicated that the PPy structure was relatively robust and the dissolution of PS microsphere was indeed feasible. Figure 8b demonstrates a TEM image showing a high resolution picture of individual hollow PPy microcapsules. The color contrast among these hollow PPy microcapsules was attributed to residual PS after THF extraction; a darker image suggested the presence of residual PS whereas a transparent image indicated the complete removal of PS. Noticeably, the PPy shell layer was mostly intact with a thickness of 20 nm (insert image in Fig. 8b).

The formation of microcapsules via the template approach is quite interesting. Currently, it has not been demonstrated yet to insert additional materials once the microcapsules are formed. According to the literature, the only feasible route to date is to design/synthesize the desirable materials as the shell layer, and after removing the core constituent, the shell layer, i.e., the microcapsules, becomes a composite [33].

In principle, the size of the PPy microcapsules could be readily adjusted by selecting PS microspheres in different sizes. In our laboratory, we are in the process of utilizing these PPy microcapsules as the substrate to support nanoparticulate IrO_2 nanoparticles for the application of biostimulating electrode to promote cell growth. We anticipate to obtain tangible data within a year and publish our results afterwards.

4 Conclusions

We developed a templated approach to fabricate uniform hollow PPy microcapsules in diameter of 527 nm with shell thickness of 20 nm. These hollow PPy

microcapsules were prepared by chemical extraction of PS from the PS@PPy microspheres. The homogeneous PS@PPy microspheres were synthesized by optimizing a water/ethanol ratio during the synthetic stage. Without the addition of ethanol, FTIR and TGA confirmed the diffusion of pyrrole molecules to the PS microspheres, engendering noticeable deformation and aggregation of PS@PPy microspheres. By optimizing the volume percentage of ethanol in an aqueous solution, proper dispersion of PS microspheres and pyrrole molecules were obtained. As a result, a desirable PS@PPy structure with significantly reduced deformation and aggregation was achieved. The PS microspheres carried negative surface charges, and after the deposition of PPy, the PS@PPy microspheres revealed a transition from positive to negative surface charges with increasing pH values.

Acknowledgements Financial supports from the Ministry of Science and Technology of Taiwan (106-2221-E-009-064; 107-2221-E-009-006-MY3; 107-2633-B-009-003; 107-2218-E-009-011) are greatly appreciated. In addition, the authors would like to thank the Ministry of Education for the funding to "Center for Neuromodulation Medical Electronics Systems" from the featured areas research center program within the framework of the higher education sprout project.

Compliance of ethical standards

Conflict of interest The authors declared that there is no conflict of interest.

References

1. Shirakawa H, Louis EJ, MacDiarmid AG et al (1977) Synthesis of electrically conducting organic polymers: halogen derivatives of polyacetylene, $(CH)_x$. J Chem Soc Chem Commun 16:578–580
2. Li Y, Wang Z, Gu H, Xue G (2011) A facile strategy for synthesis of multilayer and conductive organo-silica/polystyrene/polyaniline composite particles. J Colloid Interface Sci 355(2):269–273
3. Zhang WL, Piao SH, Choi HJ (2013) Facile and fast synthesis of polyaniline-coated poly (glycidyl methacrylate) core–shell microspheres and their electro-responsive characteristics. J Colloid Interface Sci 402:100–106
4. Lascelles SF, Armes SP (1997) Synthesis and characterization of micrometre-sized, polypyrrole-coated polystyrene latexes. J Mater Chem 7(8):1339–1347
5. Reddy KR, Park W, Sin BC et al (2009) Synthesis of electrically conductive and superparamagnetic monodispersed iron oxide-conjugated polymer composite nanoparticles by in situ chemical oxidative polymerization. J Colloid Interface Sci 335(1):34–39
6. Li W, Huang H, Li Y, Deng J (2014) Particles of polyacetylene and its derivatives: preparation and applications. Polym Chem 5(4):1107–1118
7. Choi SH, Gopalan AI, Ryu JH, Lee KP (2010) Hollow spherical nanocapsules of poly(pyrrole) as a promising support for Pt/Ru nanoparticles based catalyst. Mater Chem Phys 120:18–22
8. Wang J, Xu Y, Yan F et al (2011) Template-free prepared micro/nanostructured polypyrrole with ultrafast charging/discharging rate and long cycle life. J Power Sources 196:2373–2379
9. Su D, Zhang J, Dou S, Wang G (2015) Polypyrrole hollow nanospheres: stable cathode materials for sodium ion batteries. Chem Commun 51:16092–16095
10. Bian X, Lu X, Jin E et al (2010) Fabrication of Pt/polypyrrole hybrid hollow microspheres and their application in electrochemical biosensing towards hydrogen peroxide. Talanta 81(3):813–818
11. Mangeney C, Fertani M, Bousalem S et al (2007) Magnetic Fe_2O_3-polystyrene/PPy core/shell particles: bioreactivity and self-assembly. Langmuir 23(22):10940–10949
12. Pope MR, Armes SP, Tarcha PJ (1996) Specific activity of polypyrrole nanoparticulate immunoreagents: comparison of surface chemistry and immobilization options. Bioconjug Chem 7(4):436–444
13. Bousalem S, Benabderrahmane S, Sang YC et al (2005) Covalent immobilization of human serum albumin onto reactive polypyrrole-coated polystyrene latex particles. J Mater Chem 15(30):3109–3116
14. Fujii S, Matsuzawa S, Hamasaki H et al (2012) Polypyrrole–palladium nanocomposite coating of micrometer-sized polymer particles toward a recyclable catalyst. Langmuir 28(5):2436–2447
15. Das D, Nath B, Phukon P et al (2013) Nickel oxide/polypyrrole/silver nanocomposites with core/shell/shell structure: synthesis, characterization and their electrochemical behaviour with antimicrobial activities. Mater Chem Phys 142(1):61–69
16. Li X, He G, Han Y et al (2012) Magnetic titania-silica composite–Polypyrrole core–shell spheres and their high sensitivity toward hydrogen peroxide as electrochemical sensor. J Colloid Interface Sci 387(1):39–46
17. Zhang H, Liu Y, Wu J, Xin B (2016) One-step preparation of Fe_3O_4/Pd@polypyrrole composites with enhanced catalytic activity and stability. J Colloid Interface Sci 476:214–221
18. Li C, Zhang Y, Ji S et al (2018) Microwave absorption properties of γ-Fe_2O_3/$(SiO_2)\chi$-SO_3H/polypyrrole core/shell/shell microspheres. J Mater Sci 53:5270–5286
19. Li C, Ji S, Jiang X et al (2018) Microwave absorption by watermelon-like microspheres composed of γ-Fe_2O_3, microporous silica and polypyrrole. J Mater Sci 53:9635–9649
20. Yang F, Chu Y, Ma S et al (2006) Preparation of uniform silica/polypyrrole core/shell microspheres and polypyrrole hollow microspheres by the template of modified silica particles using different modified agents. J Colloid Interface Sci 301(2):470–478
21. Hao L, Zhu C, Chen C et al (2003) Fabrication of silica core-conductive polymer polypyrrole shell composite particles and polypyrrole capsule on monodispersed silica templates. Synth Met 139(2):391–396
22. Yao T, Lin Q, Zhang K et al (2007) Preparation of SiO_2@ polystyrene@ polypyrrole sandwich composites and hollow polypyrrole capsules with movable SiO_2 spheres inside. J Colloid Interface Sci 315(2):434–438
23. Rubinger CP, Costa LC, Esteves ACC et al (2008) Hopping conduction on PPy/SiO_2 nanocomposites obtained via in situ emulsion polymerization. J Mater Sci 43:3333–3337
24. Cheng X, Zhao Q, Yang Y et al (2010) A facile method for the synthesis of ZnS/polystyrene composite particles and ZnS hollow micro-spheres. J Mater Sci 45:777–782
25. An G, Yang C, Jin S et al (2013) Hollow TiO_2:Sm^{3+} spheres with enhanced photoluminescence fabricated by a facile method using polystyrene as template. J Mater Sci 48:5483–5488
26. Chen J, Liu Y, Li W et al (2015) Nanostructured polystyrene/polyaniline/graphene hybrid materials for electrochemical supercapacitor and Na-ion battery applications. J Mater Sci 50:5466–5474

27. Zhang H, Zhang Y, Wu C et al (2017) Preparation and photothermal study of polystyrene coated with gold nanoshell composite particles. J Mater Sci 52:6581–6590
28. Huang Z, Wang C, Li Y, Wang Z (2012) Controlled preparation of core–shell polystyrene/polypyrrole nanocomposite particles by a swelling–diffusion–interfacial polymerization method. Colloid Polym Sci 290(10):979–985
29. Cairns D, Khan M, Perruchot C et al (2003) Synthesis and characterization of polypyrrole-coated poly (alkyl methacrylate) latex particles. Chem Mater 15(1):233–239
30. Zhang J, Qiu T, Ren S et al (2012) Simple synthesis of polypyrrole–polystyrene hybrid hollow spheres. Mater Chem Phys 134(2):1072–1078
31. Han CC, Lee JT, Yang RW (1998) A new and easy method for making micrometer-sized carbon tubes. Chem Commun 19:2087–2088
32. Zhang X, Bai R (2003) Surface electric properties of polypyrrole in aqueous solutions. Langmuir 19(26):10703–10709
33. Xie C, Li P, Han L, Wang Z, Zhou T, Deng W, Wang K, Lu X (2017) Electroresponsive and cell-affinitive polydopamine/polypyrrole composite microcapsules with a dual-function of on-demand drug delivery and cell stimulation for electrical therapy. NPG Asia Mater 9:e358